Video Article

In Situ Monitoring of the Accelerated Performance Degradation of Solar Cells and Modules: A Case Study for Cu(In,Ga)Se$_2$ Solar Cells

Mirjam Theelen[1], Klaas Bakker[1], Henk Steijvers[1], Stefan Roest[2], Peter Hielkema[3], Nicolas Barreau[4], Erik Haverkamp[5,6]

[1]TNO Solliance, Thin Film Technology

[2]Eternal Sun

[3]Hielkema Testequipment

[4]Institut des Matériaux Jean Rouxel (IMN)-UMR 6502, Université de Nantes, CNRS

[5]ReRa Solutions BV

[6]Institute of Molecules and Materials, Radboud University

Correspondence to: Mirjam Theelen at mirjam.theelen@tno.nl

Abstract

The levelized cost of electricity (LCOE) of photovoltaic (PV) systems is determined by, among other factors, the PV module reliability. Better prediction of degradation mechanisms and prevention of module field failure can consequently decrease investment risks as well as increase the electricity yield. An improved knowledge level can for these reasons significantly decrease the total costs of PV electricity.

In order to better understand and minimize the degradation of PV modules, the occurring degradation mechanisms and conditions should be identified. This should preferably happen under combined stresses, since modules in the field are also simultaneously exposed to multiple stress factors. Therefore, two 'Combined Stress test with *in situ* measurement' setups have been designed and constructed. These setups allow the simultaneous use of humidity, temperature, illumination, and electrical biases as independently controlled stress factors on solar cells and minimodules. The setups also allow real-time monitoring of the electrical properties of these samples. This protocol presents these setups and describes the experimental possibilities. Moreover, results obtained with these setups are also presented: various examples about the influence of both deposition and degradation conditions on the stability of thin film Cu(In,Ga)Se$_2$ (CIGS) as well as Cu$_2$ZnSnSe$_4$ (CZTS) solar cells are described. Results on the temperature dependency of CIGS solar cells are also presented.

Video Link

The video component of this article can be found at https://www.jove.com/video/55897/

Introduction

PV systems are considered to be a cost-effective form of renewable energy. PV modules represent the core of these PV systems and are generally sold with a performance guarantee of over 25 years (*e.g.*, max. 20% efficiency loss after this period)[1]. It is crucial for the trust of consumers and investors that these guarantees are met. The electricity yield should therefore be as stable and high as possible over at least the desired module lifetime. This should be managed by reduction of both slow but steady degradation[2] and unexpected premature module failures, which, for example can occur due to production errors. Examples of observed module failures in the field are Potential Induced Degradation (PID)[3] and Light Induced Degradation (LID)[4] for crystalline silicon modules or water induced corrosion in CIGS modules[5,6,7,8]. In order to prevent a reduced field lifetime of PV modules, degradation mechanisms should therefore be identified and minimized.

Improved understanding of degradation mechanisms occurring in PV cells or modules would also help to lower PV module production costs: in many cases, protective materials against environmental stresses are introduced in modules to offer the guaranteed lifetime. This is for example true for flexible thin film modules, like CIGS, that contain an expensive barrier to prevent water ingression. All package materials in such modules can make up to 70% of the module costs. These protective materials are often over-dimensioned in order to be certain to obtain the required lifetime: more knowledge about the degradation mechanisms can therefore make solar cells more intrinsically stable and more accurately predictable. Better understanding about the long-term stability of the module and its constituents would therefore likely prevent over-dimensioning and allow reduced costs for these protective materials.

To give a general estimation of module reliability, solar cells and modules are nowadays tested and qualified by Accelerated Lifetime Tests (ALT)[9]. The most profound qualification tests are defined by the International Electrotechnical Commission (IEC) 61215 tests[10], which give "go/no go" decisions on the stability of PV modules. However, Osterwald *et al.*[11] revealed that a positive outcome of the IEC tests does not always

indicate that the PV module can stand outdoor conditions for 25 or more years. This limited correlation between field and laboratory testing was demonstrated to be especially true for the relatively new thin film modules[12].

These tests do not yield insight into the degradation mechanisms ('Which processes and/or which stresses lead to observed slow module degradation or to rapid module failure?'). Moreover, these tests, which are currently based on single or dual stress factors (for example mechanical stress, or combined temperature and humidity) can certainly not simulate field behavior in a reliable way, since PV modules in the field are subject to numerous combined stresses (for example: temperature, humidity, wind, snow, illumination, dust, sand, water). These stresses can also vary per climate zone: while in the desert, temperature and illumination are likely important stress factors; in moderate climates, the influence of for example humidity can also be very important. To simulate the degradation and consequent failures in various climates, various combinations of multiple stresses are thus required. Consequently, simultaneous exposure to multiple stresses is very important to obtain a good estimation of the module reliability in a certain climate, and combined stress tests should thus be part of laboratory tests.

It is thus proposed that qualitative and quantitative understanding of the degradation mechanisms occurring under combined stress conditions should be improved. Ideally, information about the solar cell or module should also be gathered during these tests, to allow identification of device changes during exposure. Therefore, we have designed and constructed two setups that allow simultaneous exposure to humidity, (elevated) temperatures, electrical biases, and illumination. In these setups, the severity of these stresses can also be tuned, depending on the goal of an experiment. Additionally, the illumination allows *in situ* monitoring of the PV devices (**Figure 1**)[13,14,15,16,17,18,19,20]. These types of tests will be named 'Combined Stress tests with *in situ* measurements' (CSI). In this protocol, two hybrid degradation setups, named 'CSI 1' and 'CSI 2', will be presented. Many studies, aiming at the improvement of understanding of the performance and degradation of especially thin film CIGS solar cells, were executed with these setups. A selection of stability and temperature dependency results obtained on unpackaged CIGS and CZTS solar cells are presented. More information can also be found in[21,22].
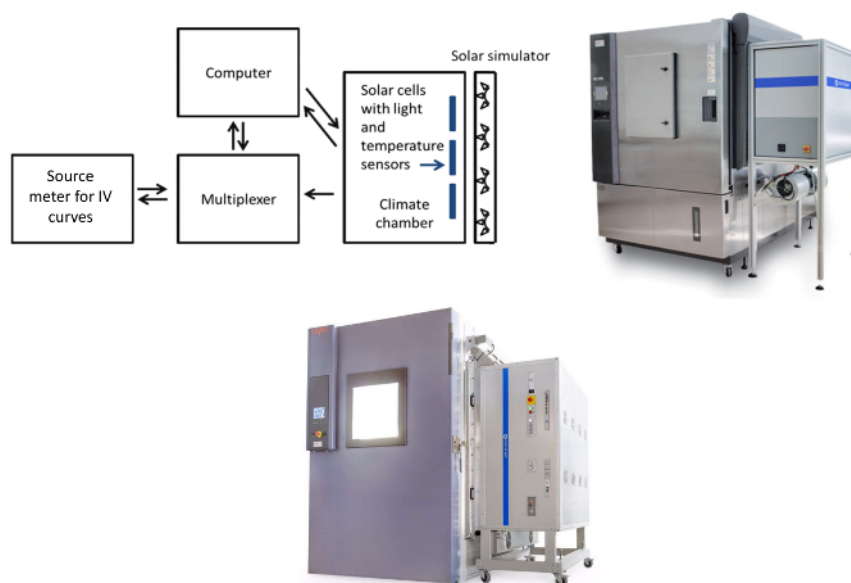

Figure 1: 'Combined Stress tests with *in situ* measurements' setup. Left: Schematic overview of a CSI setup including the measurement system. Middle and right: Photograph of the CSI setups (climate chambers plus solar simulators, measurement systems not depicted, setups have different sizes). Middle is CSI1, right is CSI2. This figure has been modified from[19,30]. Please click here to view a larger version of this figure.

Protocol

NOTE: Sections 1 and 3 are specific for degradation testing of CIGS and CZTS solar cells via this procedure, but all other types of solar cells (*e.g.*, perovskites, organic PV, and crystalline silicon) are or will be tested with these setups. It should be noted that for every device type and geometry, a sample holder should be designed. These holders should have non-corroding contacts to prevent contact degradation, since this would obscure the effects of device degradation. Moreover, it is advised to contact samples in a four-point probe configuration, to prevent the measurement of the results of corroded contacts or wires in the measurement system.

1. Preparation of CIGS Solar Cells

1. Use gloves in all steps of the protocol when handling solar cells: protect against the toxic elements, but also prevent the deposition of unwanted materials, like kitchen salt (NaCl), on the samples.
2. Cut a 1 mm x 100 mm x 100 mm soda lime (SLG) glass sample into four 100 mm x 25 mm rectangular strips with a glass cutter or diamond pen in order to prepare appropriate substrates.
3. Place the SLG sample in a sputter coater. Deposit the 0.5 µm thick molybdenum back contact by Direct Current (DC) sputtering at room temperature on the glass substrates[23].

    1. Choose from various stack sequences, including a single layer, a bilayer, and a multiplayer stack. For example, deposit a bilayer with a high initial sputtering pressure (*e.g.*, 0.03 mbar) followed by a lower sputtering pressure (*e.g.*, 0.003 mbar) at power densities of 1-5 W/cm^2.

4. Prepare an etch solution of 1 M NaOH and 0.3 M $K_3Fe(CN)_6$[24]. Electrochemically etch a 6 mm stripe of the molybdenum away to deposit a patterned back contact.
   NOTE: In this way, the solar cell has a well-defined area, without solar cell areas covered by the gold contacts, which might still partly contribute to the electrical parameters.
5. Place the sample in a vacuum chamber and deposit a 2 µm thick CIGS absorber layer by a coevaporation process under a copper, indium, gallium, and selenium atmosphere[25].
   1. For example, use typical substrate temperatures of 550 to 600 °C and follow the three-stage deposition process, first forming $(In,Ga)_2Se_3$ by evaporation of indium, gallium and selenium, followed by the formation of a copper rich CIGS due to the addition of large quantities of copper. Turn off the copper evaporator to form the required copper-poor CIGS absorber in the third stage.
   2. Alternatively, use a two-stage deposition at atmospheric pressure for a low-cost process. Perform CuInGa deposition, either by vacuum sputtering or by atmospheric pressure electrochemical deposition. Follow this by selenization under an elemental selenium atmosphere[26] in a moving belt selenization oven.

6. Place the sample in a chemical bath and deposit the CdS buffer by a "chemical bath deposition" (CBD) process with a thickness of 50 nm[27]. Typically use a water based solution of NH_4OH, $CdSO_4$, and thiourea (NH_2CSNH_2) at a temperature of ~ 70 °C.
7. Place the sample in a sputtering tool and deposit the i-ZnO/ZnO:Al front contact by Radio Frequency (RF) sputtering from i-ZnO and ZnO:Al targets with thicknesses of respectively 50 nm and 800-1,000 nm[28].
   1. For i-ZnO use a layer of a pure ZnO target and use a ZnO ceramic target with 2% Al_2O_3 for the ZnO:Al layer. Use deposition temperatures between room temperature and 200 °C. Avoid the use of a conductive metal grid in the top electrode, as this is not used in commercial modules. Therefore, use this relatively thick ZnO:Al layer to allow enough conductivity in these cells that mimic a module design.

8. Carefully scratch away a stripe of 14 mm (at the opposite side of the etching in step 1.4) of the solar cell with a knife.
   1. By making use of the difference in hardness of the layers, remove only the top layers (ZnO:Al/i-ZnO/CdS/CIGS) and leave the molybdenum back contact intact. Form solar cells with a width of 5 mm, similar to the width of a cell in a module.

9. Place the sample in a gold sputtering tool and cover it with a stripe in the middle as a mask, so that no gold is deposited on the solar cell. Deposit gold contacts of ~ 60 nm thickness by sputtering at room temperature on both the back contact (molybdenum) and the front contact (ZnO:Al) in order to allow contacting of the cells.
   NOTE: The use of a contact of a noble metal allows long term exposure of the samples to harsh conditions without degradation of the contacts, so that the cell degradation can be studied.
10. Cut the strips with a glass cutter or a diamond pen into 7 mm wide samples, that now have a cell surface of ~ 7 mm x 5 mm and a total size of 7 mm x 25 mm (**Figure 2**).
    Note: A schematic representation of the cross-section as well as a microscopy picture of a cell is shown in **Figure 2**. For the experiments with CZTS solar cells, a different deposition procedure of the active absorber layer (CZTS) has been followed (similar to reference[29]), while all other layers were deposited following an analog procedure.
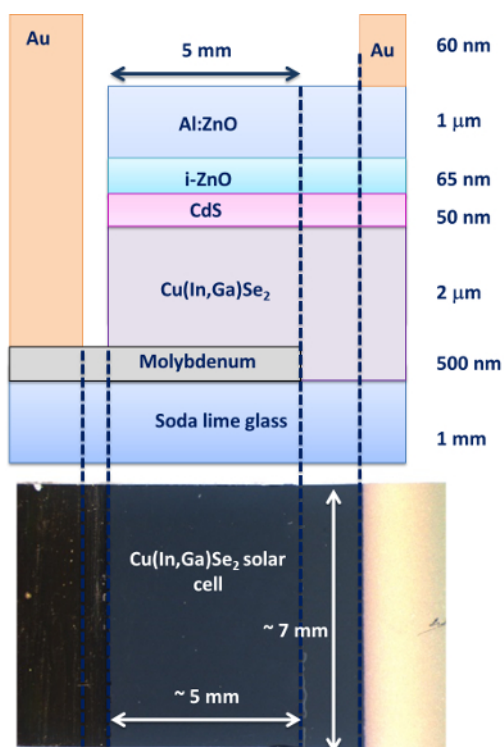
Figure 2: CIGS sample design. (top) Schematic representation of the cross-section of a CIGS sample and (bottom) a microscope picture of a CIGS sample taken from the top. This figure has been partly modified from references[14,30]. Please click here to view a larger version of this figure.

2. Analysis of the Solar Cells Before Degradation

1. Measure the *ex situ* current voltage (IV) performance of the solar cells under standard test conditions (STC, illumination: 1000 W/m² and AM 1.5, temperature: 25°C) in a four point probe configuration to determine the electrical parameters with an IV tester.
   1. Measure the external quantum efficiency (EQE) for the exact current density and wavelength dependent absorption[30,31] with a spectral response (SR) setup and calculate the exact current density.

2. Record the illuminated lock-in thermography (ILIT) mapping[31] and the photoluminescence (PL) mapping[31] with a large magnification and take (microscopy) images to identify any visual and lateral defects.
   1. Place the sample under an ILIT device with heat detector with a 15 μm lens for high magnification and an IR illumination source. Illuminate the sample and record the spatial difference in temperature to identify the heated locations.
   2. Place the sample under a mapping PL setup to obtain a spatial photoluminescence image. Use a high power LED light source for illumination and a CCD camera for data detection.
      NOTE: Examples can be found in references[15,16,20,30].

3. Select a number of solar cells for the degradation experiment, while placing the rest of the samples in an argon glovebox as reference. Select a mixed set of solar cells as reference and as experimental samples, so any difference within the full slides (e.g. gradients in composition) are in the same severity present in the experiment and reference samples.
   NOTE: This could for example mean that cells with positions 1, 3, 4, 5, 7 and 8 on the slides are experimental cells, while positions 2 and 6 are reference cells.

3. Placement of the Solar Cells into Sample Holders

1. Place the solar cells in sample holders that do not cast any shadow on the cells and make contact between the gold front and back contacts and measurement pins.
   NOTE: The sample holders are specifically designed to withstand the harsh conditions during the climate tests. Moreover, they are constructed of materials that have only limited outgassing.
2. Place the sample holders on the sample rack inside the CSI setup, which allow electrical contact between the solar cells and the measurement tools outside the setup. Place the sample rack on the dedicated position, where it will be illuminated by an AM 1.5 light source.
   NOTE: Light source specifications are as follows. CSI1: 40 cm x 40 cm area, 1,000 W/m², BAA calibrated illumination; CSI2: 100 x 100 cm² area, 1,000 W/m², AAA calibrated illumination, calibrations according to IEC60904-9:2007[32].

4. Execution of the Degradation Experiment

1. Switch on the solar simulator, the measurement equipment, the climate chamber, and the computer.
2. Program the measurement computer, which controls the solar simulator, electrical biases, and climate chamber settings. Define the voltage range, voltage steps, measurement sequence, and time between the measurements in the IV measurement software, and define temperature, humidity, bias voltage, and illumination profiles in the software.
   NOTE: Let this software steer the measurements during the full experiment.
   1. For typical settings for the IV measurements, use voltage in the range -0.2 V to +1.0 V in 120 steps (0.01 V/step). Note that in most cases, the system alternates between the IV measurements of all samples and pauses of around 5 min.

3. Stabilize the temperature of the climate chamber and the solar cells in the setup. Observe the sample temperature in the software.
   NOTE: A typical temperature for the solar cells is 25 °C, which is the STC temperature. Since the illumination heats up the samples, the sample temperature is always higher than the surrounding chamber. Typical starting temperatures of the climate chamber are -10 °C to +5 °C (+5 °C chamber temperature can for example lead to CIGS sample temperatures of 25 °C). If other sample designs or compositions are selected, other chamber temperatures can be required to obtain 25 °C sample temperature.
4. Heat the climate chamber slowly until it reaches 85 °C, for example at 0.1-0.3 °C/min. Read the chamber temperature from the climate chamber computer and read the sample temperature from the software.
   NOTE: Typical samples temperatures are then between 100 °C and 110 °C when the chamber is 85 °C. These values vary between samples, and are especially influenced by the substrate type, the sample holder design and material, and the solar cell itself. During this stage, the cells are in open circuit conditions when they are not measured, unless mentioned differently. If the influence of any internal voltage bias during the heating stage has to be excluded, the illumination can also be off during this stage.
   1. For CSI1, attach an individual thermocouple to all individual cells to measure their temperature, while in CSI2 use 15 thermocouples for 32 samples. Record and log the individual temperatures.

5. Automatically measure the current voltage curves of the solar cells one by one during the heating, which means that they are determined every 0.5 to several min, depending on the number of samples. Observe the electrical parameters in the software.
   1. Calculate the electrical parameters from the current voltage curves. Always determine the efficiency, open circuit voltage, short circuit current density, fill factor, series resistance, and shunt resistance. Determine the resistances from the slopes on the end of the current voltage curves.
   2. If required, also determine the ideality factor, saturation current density, and photo current density by fitting with the one-diode model[14].
      NOTE: However, note that these fitting procedures are relatively unreliable for degraded solar cells that do not behave like ideal diodes. The efficiency as measured by these elevated temperatures will be lower than under STC, which is mostly visible in a decrease in the open circuit voltage[13].

6. Turn on the humidity in the climate chamber, a standard setting is a relative humidity (RH) of 85%. This is generally the starting point of the experiment (t = 0 h). Observe the RH from the climate chamber computer.
   NOTE: The actual sample relative humidity is lower than the set value. This is caused by the fact that the sample temperature is higher than 85 °C, while the absolute humidity is the same: since the relative humidity is a function of the temperature, this value is lower than 85% RH[33].

7. Leave the samples in the CSI setups for 100s to 1,000s of hours, while measuring the current voltage curves. Measure the curves every 5 to 10 min, but vary this on demand. Observe the electrical parameters in the software.
   1. In the remaining time, keep the samples either under open circuit conditions (standard conditions) or place them under various electrical biases with the use of electrical loads, varying from -20 V to +20 V. In case a modification of the electrical bias is required during the experiment, change the set value in the tracer software.
      NOTE: 'Standard' settings are the maximum power point (MPP) conditions (the operation voltage and current of a solar cell), short circuit conditions, and conditions with a limited negative voltage. Use the latter to simulate partial module shading.

8. To learn more about samples after various exposure times, remove a limited number of samples in the sample holders from the setup before the others. Execute this under illumination and in a very rapid manner in order to minimize the influence on the remaining samples. This is naturally only possible for small samples.

9. At the end of the experiment, cool the chamber down to room temperature slowly in a few hours and remove the samples together with their sample holders. Observe the temperature from the climate chamber computer.
   NOTE: It is also possible to use other light intensities (*e.g.*, 800 W/m^2 or ultraviolet light), while the humidity and temperature can naturally also be varied. In that case, the obtained electrical parameters should be corrected for the different light intensity. It was observed that unexpected changes in electrical parameters occurred when CIGS solar cells were shortly (*e.g.*, 15 min) not illuminated (and heated by the illumination source). If this effect is not the aim of the study, it is recommended to leave on the illumination continuously[14].

5. Analysis of Degraded and Reference Cells

1. Plot the development of the electrical parameters as a function of exposure time in the degradation setups.
2. Repeat the *ex situ* IV measurements of the degraded solar cells directly after the samples are removed from the setups to obtain the electrical parameters at STC. Repeat the external quantum efficiency measurements for the exact current density and wavelength-dependent absorption.
3. Record again the illuminated lock-in thermography mapping and photoluminescence mapping, and take (microscopy) pictures to identify any change in visual and lateral defects. Use the same settings as before degradation.
4. Use other analysis techniques, like (cross-section) Scanning Electron Microscope-Energy Dispersive X-ray spectroscopy (SEM-EDX)[31], X-Ray Diffraction (XRD)[31], Secondary Ion Mass Spectroscopy (SIMS)[31], and temperature dependent current voltage (IV(T))[31] to further identify the failure mechanisms.
   1. Execute these destructive analyses on both degraded and reference samples to observe the changes due to exposure in the CSI setups.

6. Definition of the Degradation Mechanisms and Modes

1. Combine all the data to define degradation mechanisms and their impact on long term stability of the solar cells or modules.

Representative Results

The CSI setups have been used for a wide range of experiments. Experiments have both focused on the influence on the cell or module composition and design, as well as on the influence of the degradation conditions. Some examples of the development of electrical parameters are displayed in the following figures. Measurements in **Figure 3**, **Figure 5**, **Figure 6**, and **Figure 7** were taken in CSI1, while **Figure 4** was obtained in CSI2. In these figures, it is chosen to depict either the device efficiency, the open circuit voltage, or the shunt resistance, but other parameters can naturally also be plotted.

Figure 3 and **Figure 4** display the influence of the degradation conditions on stability of alkali-rich CIGS solar cells without a humidity barrier or any other package material. **Figure 3** shows that these cells degrade when they are exposed to illumination, heat, and humidity, while they are almost stable in the absence of humidity. This indicates that these solar cells or analog modules might be completely stable when well packaged against humidity[15]. Potential package materials naturally include glass, but also flexible barriers, which are often based on organic-inorganic multi-stacks[15]. In future experiments, these possibilities will also be tested. These results also indicate that this package material might not be necessary in a hot and dry climate. **Figure 4** shows the influence of a bias voltage when exposed to damp heat plus illumination: these preliminary results indicate that a low negative voltage (-0.5 V, grey curves) likely has a more negative effect on stability than short circuit, open circuit, and MPP conditions[18].
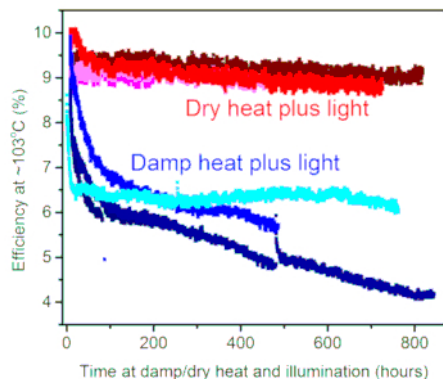
Figure 3: Influence of humidity on CIGS solar cell stability. The development of the efficiency of unpackaged CIGS solar cells as a function of exposure time to illumination plus dry heat (red) and damp heat (blue) taken at elevated temperatures. Every line represents one solar cell. This figure has been modified from reference[15]. Please click here to view a larger version of this figure.
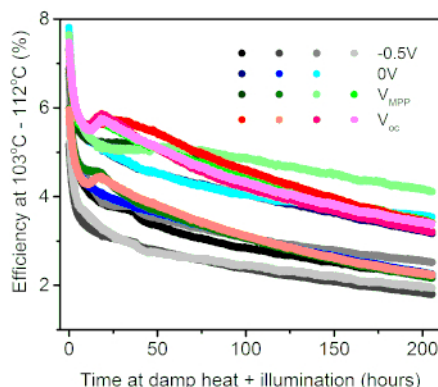

Figure 4: Influence of electrical loads on CIGS solar cell stability. Evolution of the efficiency of unpackaged cells as a function of time at various voltages plus damp heat and illumination. Grey, blue, green, and red curves indicate exposure to -0.5 V, 0 V, ~ V_{MPP}, and open circuit conditions, respectively. These parameters are obtained at elevated temperatures, while the room temperature efficiencies are around 50% higher. Every line represents one solar cell. This figure has been modified from reference[18]. Please click here to view a larger version of this figure.

Due to the slow heating (0.1-0.3 °C/min) during the heating phase and the real-time measurements, these setups also automatically allow the determination of the temperature dependency of solar cells. **Figure 5** displays the dependency of the open circuit voltages as obtained from the heating curves before degradation experiments. This graph shows that differences exist between the open circuit voltage (V_{oc}) temperature dependency of various CIGS solar cells, while other parameters like the series resistance and the short circuit current (not depicted) display even larger differences between cells. The development of other parameters can be found in reference[34].
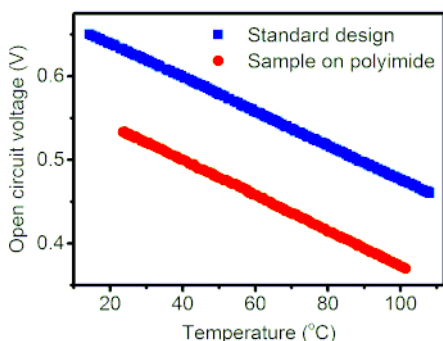

Figure 5: Temperature dependency of CIGS solar cells. Temperature dependency of the open circuit voltage (V_{oc}) of two unpackaged CIGS solar cells. The colors indicate different solar cell designs: the blue squares represent samples with the cell design and deposition procedure as described above. The red circles indicate a non-packaged CIGS solar cell on polyimide foil with absorbers deposited with ion-beam assisted coevaporation. Every line represents one solar cell. This figure has been modified from reference[34]. Please click here to view a larger version of this figure.

Figure 6 shows that small differences in the composition of solar cells can have a large influence on the device stability. This experiment demonstrated that alkali-rich samples containing large quantities of sodium and potassium had a higher initial efficiency, but they also degraded more rapidly. On the other hand, almost stable unpackaged solar cells that only contained small quantities of alkali-elements ("alkali-poor" samples) were also produced. These solar cells were thus almost intrinsically stable and did not need any protective material. Based on this information combined with *ex situ* analysis results, the main degradation mechanisms for these samples could be identified: it was observed that the main driver behind the efficiency-loss of the alkali-rich samples was a sharp decrease in shunt resistance[16]. In-depth analysis of the properties of these cells displayed that the migration of alkali-elements, more specifically sodium, seemed to cause this decrease. More information is presented in references[16,20]. Later stages of this study aim to develop solar cells with the stability of the alkali-poor samples, and the high initial efficiency of the alkali-rich samples.
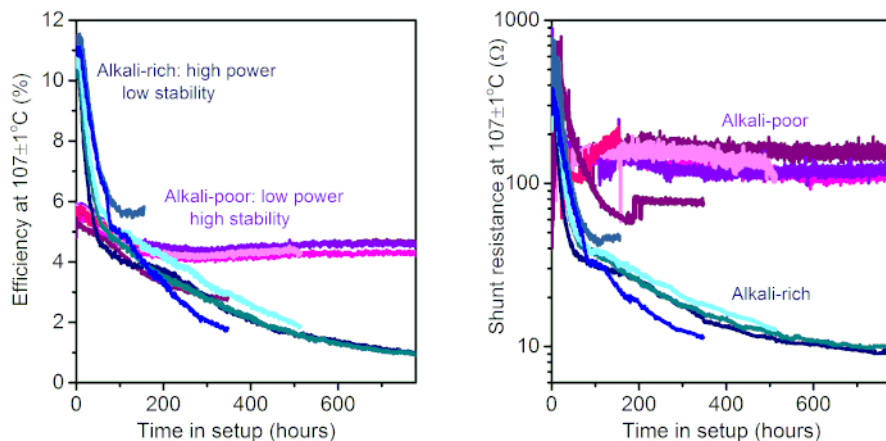

Figure 6: Influence of the alkali-content on CIGS solar cell stability. Evolution of the efficiency (left) and shunt resistance (right) of two types of unpackaged CIGS solar cells exposed to damp heat plus illumination. The pink and purple lines represent the alkali-poor samples, while the blue lines represent the alkali-rich samples. The values were obtained at elevated temperatures, while room temperature efficiencies are 30-80% higher. Every line represents one solar cell. This figure has been modified from reference[16]. Please click here to view a larger version of this figure.

A last example focuses on various CZTS samples[19]. **Figure 7** shows that different types of unpackaged solar cells demonstrate a different IV behavior under damp heat plus illumination. It should be noted that these cells are not ideal solar cells, so the increase in efficiency and voltage as displayed in this figure is likely not representative for CZTS solar cells in general and no explanation could be provided for this behavior. More studies need to be executed to give reliable statements about the stability of these cells.
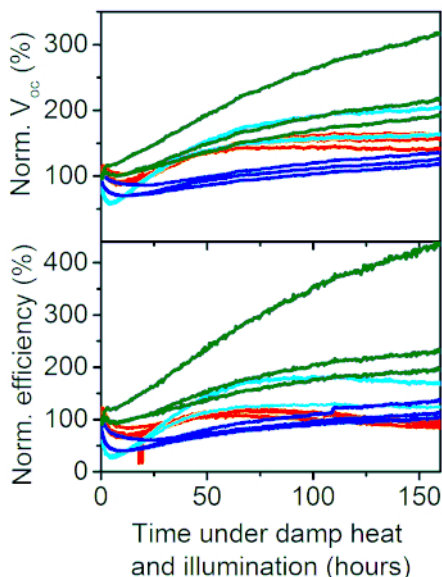

Figure 7: CZTS solar cells exposed to damp heat plus illumination. Evolution of normalized open circuit voltage and efficiency of four types of non-optimized unpackaged CZTS solar cells as a function of time, exposed to damp heat plus illumination taken at elevated temperatures. Every color depicts a different type of CZTS solar cell. Every line represents one solar cell. This figure has been modified from reference[19]. Please click here to view a larger version of this figure.

Discussion

Two CSI setups for real-time monitoring of the electrical parameters of solar cells and modules have been designed and constructed. These setups allow simultaneous exposure to damp heat, illumination, and electrical biases, while also *in situ* determining the IV parameters of PV devices. These setups have been used to study the influence of environmental stresses (humidity, illumination, electrical biases, and temperature) as well as cell or module composition on the long-term stability of unpackaged solar cells. **Figure 3**, **Figure 4**, **Figure 5**, **Figure 6**, and **Figure 7** display a selection of results obtained with these setups.

Stability results (**Figure 3**, **Figure 4**, **Figure 6**, and **Figure 7**) from the presented studies should always be treated with care: in order to make the translation from these studies to module stability, the constraints of all accelerated lifetime tests on the stability of PV devices (including this study) should be taken into account. These constraints are caused by the fact that the conditions in the laboratory are meant to rapidly identify degradation mechanisms, while some degradation mechanisms might not be found due to the selection of the wrong (severity of) stresses. Moreover, the chosen conditions might also lead to degradation mechanisms and consequent failures that do not occur in the field or occur in the field before or after the predicted time frame. While for example for damp heat conditions (85 °C/85% RH), an acceleration factor of 219 is assumed, reference[25] showed that this rate is often non-linear and can vary in CIGS modules between 10 and 1,000, and for different degradation mechanisms.

To estimate the validity of the presented results, the most important differences between the field module exposure and the presented experiments should be taken into account:

a. Used laboratory conditions are more severe than field conditions, which is an intrinsic requirement for accelerated testing. Moreover, the conditions in these experiments are mostly constant, while modules in the field will be exposed to continuously changing conditions.

b. In the presented experiments, non-packaged solar cells were used. Naturally, barrier materials and edge sealants will play an important role in the device stability (especially under humid conditions). Additionally, the influence of interconnection and encapsulation materials is also very important and should not be neglected. Certainly, experiments with packaged and interconnected mini-modules are also possible in these setups.

c. Due to the illumination, the experiments presented in **Figure 3**, **Figure 5**, **Figure 6**, and **Figure 7** were executed under open circuit conditions when the IV curves were not recorded. However, modules should function under MPP conditions, while the cells could also be exposed to reversed bias conditions in the case of partial module shadowing. **Figure 4** shows that only limited differences between MPP and open circuit conditions were observed in that specific experiment, but that might be different for other cells or conditions.

d. The composition of the CIGS solar cells has a large influence on the long-term stability. Examples of studies on the influence of the composition on the stability can for example be found in references[16,20]. Since the exact nature of the influence of many small modifications in the solar cell stack is not yet identified, degradation might occur faster or slower than expected.

The above factors indicate that a large number of accelerated lifetime studies with variation in degradation conditions and sample composition is required to truly predict module field performance. Moreover, these results should therefore be combined with field studies to obtain a complete picture about the long-term stability of PV modules.

However, we propose that the setups presented in this study are substantial improvements compared to the standard IEC tests, due to the combined stress exposure as well as *in situ* monitoring. These properties greatly improve the predictive value of accelerated lifetime experiments and increase our understanding of degradation mechanisms. The four main advantages compared to 'standard' (*e.g.*, IEC 61215) tests are the following capabilities:

a. Testing under exposure to combined stresses (*i.e.*, temperature, humidity, illumination, and electrical biases).

b. Tuning of combined stresses in order to simulate local climates (*e.g.*, desert or polar conditions).

c. Tuning of electrical biases, *e.g.*, to simulate effects of partial shading.

d. Real-time monitoring of the device performance, allowing simpler and faster testing as well as better prediction or limitation of the degradation mechanisms due to an increased knowledge level.

e. Reduced testing time, since a test can be stopped directly after a failure has occurred, instead of after the defined test period (*e.g.*, 1,000 h).

It is therefore proposed that lifetime studies with the presented setups can greatly improve the qualitative and quantitative understanding and prediction of long-term stability of solar cells and modules. In the future, a setup offering 'Combined Stress tests with *in situ* measurements' (CSI) for full scale modules will be developed: the setups with illuminated areas of 40 cm x 40 cm and 100 cm x 100 cm are too small for full-size PV modules, so plans to increase the scale of this combined stress measurement concept are underway.

Disclosures

The authors Erik Haverkamp (ReRa Solutions), Stefan Roest (Eternal Sun), and Peter Hielkema (Hielkema Testequipment) are employed by the consortium commercializing these setups. The employer of the inventors of these setups (authors Mirjam Theelen and Henk Steijvers (TNO)) holds a license agreement with this consortium.

Acknowledgements

References

1. Jordan, D., Kurtz, S., VanSant, K., Newmiller, J., Compendium of Photovoltaic degradation rates, *Prog. Photovolt.* **24** (7), 978-989, (2016).
2. Pingel, S. et al., Potential induced degradation of solar cells and panels, *Proc. 35th IEEE PVSC.* 2817-2822 (2010).
3. Lindroos, J., Savin, H., Review of light-induced degradation in crystalline silicon solar cells, *Sol. Energ. Mat. Sol. Cells.* **147,** 115-126 (2016).
4. Theelen, M., Daume., F., Stability of Cu(In,Ga)Se$_2$ solar cells: A literature review, *Solar Energy.* **133,** 586-627 (2016).
5. Malmström, J., Wennerberg, J., Stolt, L., A study of the influence of the Ga content on the long-term stability of Cu(In,Ga)Se$_2$ thin film solar cells, *Thin Solid Films.* **431 - 432,** 436-442 (2003).
6. Wennerberg, J., Kessler, J., Stolt, L., Degradation mechanisms of Cu(In,Ga)Se$_2$-based thin film PV modules, *Proc. 16th EUPVSEC.* 309-312 (2000).
7. Feist, R., Rozeveld, S., Kern, B., D'Archangel, J., Yeung, S., Bernius, M., Further investigation of the lifetime-limiting failure mechanisms of CIGSS-based minimodules under environmental stress, *Proc. 34th IEEE PVSC.* 2359-2363 (2009).
8. Sharma, V., Chandel, S., Performance and degradation analysis for long term reliability of solar photovoltaic systems: A review, *Renew. Sustainable Energy Rev.* **27,** 753-767(2013).
9. PV Module Certification for new Standards and new Technologies, *Fraunhofer ISE.* https://www.ise.fraunhofer.de/content/dam/ise/de/documents/infomaterial/brochures/photovoltaik/flyer-pv-module-certification-for-new-standards-and-new-technologies.pdf accessed 19-3-2017 (2017).
10. Osterwald, C., McMahon, T., History of Accelerated and Qualification Testing of Terrestrial Photovoltaic Modules: A Literature Review, *Prog. Photovolt.* **17,** 11-33 (2009).
11. Carlsson, T., Brinkman, A., Identification of degradation mechanisms in field-tested CdTe modules, *Prog. Photovolt.* **14,** 213 - 224 (2006).
12. Jordan, D., Kurtz, S., VanSant, K., Newmiller, J., Compendium of photovoltaic degradation rates, *Prog. Photovolt.* **24,** 978-989 (2016).
13. Theelen, M., Tomassini, M., Steijvers, H., Vroon, Z., Barreau, N., Zeman, M., In situ Analysis of the Degradation of Cu(In,Ga)Se$_2$ Solar Cells, *Proc. 39th IEEE PVSC.* 2047-2051 (2013).
14. Theelen, M. et al., Accelerated performance degradation of CIGS solar cell determined by in situ monitoring, *Proc. SPIE 9179.,* 91790I (2014).
15. Theelen, M., Beyeler, K., Steijvers, H., Barreau, N., Stability of CIGS Solar Cells under Illumination with Damp Heat and Dry Heat: A Comparison, *Sol. Energ. Mat. Sol. Cells.* **166,** 262-268 (2017).
16. Theelen, M., Hans, V., Barreau, N., Steijvers, H., Vroon, Z., Zeman, M., The impact of sodium and potassium on the degradation of CIGS solar cells, *Prog. Photovolt.* **23,** 537-545 (2015).
17. Theelen, M., Hendrikx, R., Barreau, N., Steijvers, H., Böttger, A., The effect of damp heat - illumination exposure on CIGS solar cells: a combined XRD and electrical characterization study, *Sol. Energ. Mat. Sol. Cells.* **157,** 943-952 (2016).
18. Theelen, M. et al., The Exposure of CIGS Solar Cells to Different Electrical Biases in a Damp-heat Illumination Environment, *Proc 43rd IEEE PVSC.* 0929-0934(2016).
19. Theelen, M. et al., In situ monitoring of the accelerated performance degradation of thin film solar cells, *Proc. 42th IEEE PVSC.* 1-6, (2015).
20. Theelen, M., Barreau, N., Steijvers, H., Hans, V., Vroon, Z., Zeman, M., Degradation of CIGS solar cells due to the migration of alkali elements, *Proc. 42th IEEE PVSC.* 1-6 (2015).
21. *In situ monitoring of the degradation of CIGS solar cells.* https://www.youtube.com/watch?v=Zmy5tb-2NK8, accessed on March 15th (2017).
22. *Hybrid degradation testing of solar cells and modules.* https://www.youtube.com/watch?v=tEsvkTco-To, accessed on March 15th (2017).
23. Theelen, M. et al, Influence of Mo/MoSe$_2$ microstructure on the damp heat stability of the Cu(In,Ga)Se$_2$ back contact molybdenum, *Thin Solid Films.* **612,** 381-392,(2016).
24. Hovestad, A, Bressers, P., Meertens, R., Frijters, C., Voorthuijzen, W., Electrochemical etching of molybdenum for shunt removal in thin film solar cells, *J. Appl. Electrochem.* **45** (7), 745-753, (2015).
25. Couzinie-Devy, F., Barreau, N., Kessler, J., Re-investigation of preferential orientation of Cu(In,Ga)Se$_2$ thin films grown by the three-stage process, *Prog. Photovolt.* **19,** 527-536, (2011).
26. Schmidt, S. et al., Adjusting the Ga grading during fast atmospheric processing of Cu(In,Ga)Se$_2$ solar cell absorber layers using elemental selenium vapor, accepted in *Prog. Photovolt.* **25** (5), 341-357 (2017).
27. Contreras, M. et al., Optimization of CBD CdS process in high-efficiency Cu(In,Ga)Se$_2$-based solar cells, *Thin Solid Films.* **403-404,** 204-211 (2002).
28. Theelen, M., et al., Physical and chemical degradation behavior of sputtered aluminum doped zinc oxide layers for Cu(In,Ga)Se$_2$ solar cells, *Thin Solid Films.* **550,** 530-540 (2014).
29. Brammertz, G. et al., Characterization of defects in 9.7% efficient Cu$_2$ZnSnSe$_4$-CdS-ZnO solar cells, *Appl. Phys. Lett.* **103** (16), 163904 (2013).
30. Theelen, M., *Degradation of CIGS solar cells.* Ipskamp Drukkers. (2015).
31. Abou-Ras, D., Kirchartz, T., Rau, U., *Advanced Characterization Techniques for Thin Film Solar Cells.* Wiley-VCH (2011).

32. Wolhgemuth, J., Standards for PV Modules and Components - Recent Developments and Challenges, *Proc. 27th EUPVSEC.* 2976 - 2980 (2012).
33. *Hyperphysics Relative Humidity.* http://hyperphysics.phy-astr.gsu.edu/hbase/kinetic/relhum.html, accessed 19-3-2017 (2017).
34. Theelen, M. et al., Temperature Dependency of CIGS solar cells on soda lime glass and polyimide: a comparison. accepted to *JRSE.* (2016).
35. Coyle, D., Life prediction for CIGS solar modules part 1: modelling moisture ingress and degradation, *Prog. Photovolt.* **21** (2), 156-172, (2013).